Monitoring gas hydrates under multiphase flow in a high pressure flow loop by means of an acoustic emission technology

Vinicius R. de Almeida, Eric Serris, Ana Cameirão, Jean-Michel Herri, Emilie Abadie, Philippe Glenat

Version of Record: https://www.sciencedirect.com/science/article/pii/S1875510021005333
Manuscript_cfa0335d2f86954abe3ce3fc0001c28c

Monitoring gas hydrates under multiphase flow in a high pressure flow loop by means of an acoustic emission technology

Vinicius DE ALMEIDA[1,*], Eric SERRIS[1], Ana CAMEIRAO[1], Jean-Michel HERRI[1], Emilie ABADIE[2], Philippe GLENAT[2]
[1]Ecole des Mines de Saint-Etienne, SPIN Centre, Saint-Etienne, France
[2]TotalEnergies - CSTJF, Pau, France

*Corresponding author: vinicius.de-almeida@emse.fr (V. De Almeida)

ABSTRACT

The formation of natural gas hydrates in oil and gas pipelines is an important concern due to the risk of hydrate blockage. In order to reduce the expenses with the use of chemicals to avoid hydrate plugging, more studies about the slurry flow and the mechanisms of blockage in flowing conditions are necessary. In this study, it is presented an experimental work combined with a multi-instrumental data analysis to allow monitoring hydrate formation and track the particles in time and space. Acoustic emission (AE) is used in a high pressure flow loop apparatus to capture acoustic waves generated by the flow and to detect the presence of hydrates flowing in the system. The tests are conducted with Kerdane oil, saline water and natural gas at 75 bar and 4 °C. Two tests are presented, one at 30 and another at 80% water cut (water fraction in volume). It is shown that, with the absolute energy obtained from the AE sensors, it was possible to detect the beginning of hydrate crystallization and the hydrates displacement in the pipeline, because the absolute energy increases as the collisions of particles generate more acoustic emission. The results show that, for the tests performed, the flow became heterogeneous after hydrate formation, with some regions of the flowing volume containing more hydrates than others. It is also shown that the non-flowing volume of hydrates with entrapped liquid, caused by deposition or settling, can be estimated with AE.

Keywords: natural gas hydrates, tracking hydrate particles, acoustic emission, oil-water dispersions, flow loop experiments.

1. Introduction

Ensuring the safe multiphase transport in offshore petroleum pipelines can be a challenge in flow assurance, mainly due to gas hydrate crystallization. The delivery of all the drained liquid extracted from

the reservoir to the topside separator is often threatened by hydrate crystallization because the solid particles may plug the system (Sloan and Koh, 2008; Sloan et al., 2011; Cardoso et al., 2014). There are two main strategies used by the industry to avoid hydrate blockage: hydrate avoidance and hydrate management. The first one consists in a complete hydrate avoidance by means of thermodynamics (Nasir et al., 2020; Qasim et al., 2020; Deka et al., 2021). The second strategy consists in accepting hydrate formation as long as hydrates transport is stable and offers no risk to the production (Sloan, 2005; Kinnari et al., 2015; Olajire, 2020). Hydrate management is preferred in terms of costs, but there are uncertainties about its safety in many scenarios. The extension of the hydrate management strategy to more critical conditions requires a better understanding about the mechanisms of hydrate formation and plugging under flowing conditions, and this is still a challenge even in laboratory tests.

Flow loops are experimental pilots that can be used to study hydrate particles formation under flow and to understand the mechanisms of deposition, agglomeration and plugging (Fidel-Dufour et al., 2006; Joshi et al., 2013; Yan et al., 2014; Melchuna et al., 2016; Aman et al., 2016; Ding et al., 2016; Pham, 2018; Liu et al., 2019; Liu et al., 2020; Liu et al., 2021). A common procedure in experiments with hydrates is to monitor temperature and gas consumption to know when the crystals are forming and to estimate the hydrate fraction and water conversion. The presence of hydrates often causes variations in pressure drop, density and flow rate as well. Despite many recent advancements in measurements and visualizations presented in the literature, the size of this type of apparatus brings challenges in terms of monitoring hydrate crystallization and tracking the particles in time and space.

Acoustic emission (AE) is a promising non-intrusive technology that can be used to track hydrates in flowing systems. AE was previously used to monitor pharmaceutic crystallization process (Gherras et al., 2012), to characterize the flow noise in gas-liquid flows (Fang et al., 2013), to monitor slug flow (Al-Lababidi et al., 2012), to identify the flow pattern in two-phase flow (Husin et al., 2013), for application in gas-solid flows (Hii et al., 2013), to detect the presence of sand and droplets in pipelines (El-Alej et al., 2013; El-Alej et al., 2014), to study the impact of abrasive particle in a slurry flow (Droubi et al., 2015; Droubi and Reuben, 2016), among others. The first application of AE in flow loop tests with gas hydrates was presented by Cameirao et al. (2018), showing the potential of this technique to monitor the beginning of crystallization, agglomeration, and plug/sedimentation.

In this work, the absolute energy obtained from AE measurement is used to detect gas hydrates flowing in a pipeline and to obtain the spatial distribution of particles. The procedure here is to analyze the trend of the absolute energy before and after hydrate formation and to follow the evolution of the

signals as hydrates form. Another important application of the technique is to estimate hydrate deposition or accumulation in singularities of the system.

2. Experimental methodology for monitoring gas hydrates in a flow loop

2.1 Flow loop description

The Archimede flow loop, illustrated in Figure 1, is a pipeline of 56 meters for circulating liquid under high pressure and controlled temperature. It is composed by a separator, at the top of the flow loop, where the natural gas is injected and there is contact between the circulating liquid and the gas. The injection of gas can be fast and manual or slow with an automatic injection with a gas flow meter. The pipeline is divided into three sections: a vertical downward section of approximately 9.5 meters, a slightly downward section (inclination of -3.6°) of approximately 36 meters and a vertical upward section of approximately 10.5 meters. The vertical sections have a pipe diameter of 15.7 mm, while the slightly inclined section has a pipe diameter of 10.2 mm. The power for circulating the liquid is provided by a Moineau pump with a flow capacity ranging between 100-500 L/h (which corresponds to 0.14-1.70 m/s).

The apparatus has a total of ten temperature probes (with a span of 0.1 °C) whose one measures the room temperature, two absolute pressure probes (one for the separator and another one for the gas injection system, with an span of 0.01 bar), four differential pressure probes (Δp_1, Δp_2 and $\Delta p_3$with an uncertainty of 120 Pa±2.5×10^{-4}p, Δp_4 with an uncertainty of 10 Pa ± 2.5×10^{-4}p), an automatic gas injection with a gas flow meter (minimum span of 0.01 ln/minute), and a Coriolis that measures the density (with an uncertainty of ±2.0 kg/m^3) and the flow rate of the liquid that circulates in the loop (uncertainty of 0.2%).

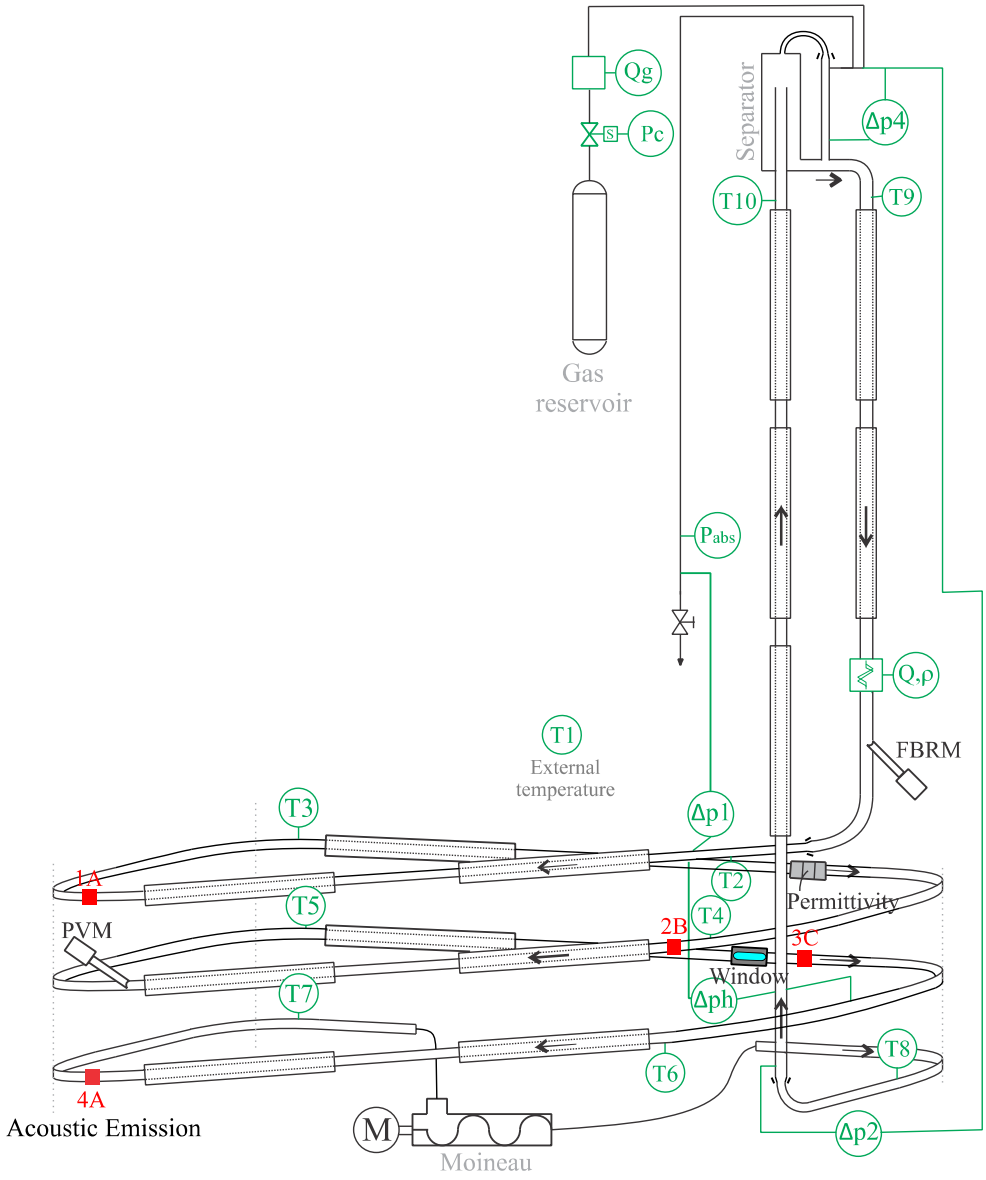

Figure 1. Schematic illustration of the Archimede flow loop.

The pilot is also equipped with two *in situ* probes: a Focused Beam Reflectance Measurement (FBRM) installed in the downward section, and a Particle Vision and Measurement (PVM) in the slightly inclined section. These two instruments give information of the flow pattern and chord length distribution at microscopic scale (Melchuna et al., 2016; Pham, 2018). From the FBRM, it is obtained the chord counts distribution in a range 1-1000 µm. From the PVM, it is obtained images of the flow in a range 1075-825 µm and the grayscale of the images. In addition, the Archimede flow loop has been upgraded with the installation of AE sensors, a permittivity probe and a high-speed camera.

2.2 Acoustic emission testing

Acoustic emission is the appearance of transient acoustic waves due to a change in the system. For the experiments carried out in the Archimede flow loop, it captures the acoustic emission produced by the flow inside the pipe, as part of the energy dissipated due to shear and particle-particle and particles-wall collisions is converted to acoustic energy. The appearance of hydrates is expected to produce more noise than before hydrate formation. Each sensor is fixed outside of the pipe and it is a non-intrusive measurement, as illustrated in Figure 2. The acoustic waves captured by a sensor can be converted to absolute energy, amplitude, counts and many other parameters. For this work, it is analyzed only the absolute energy, which is measured each 0.5 second.

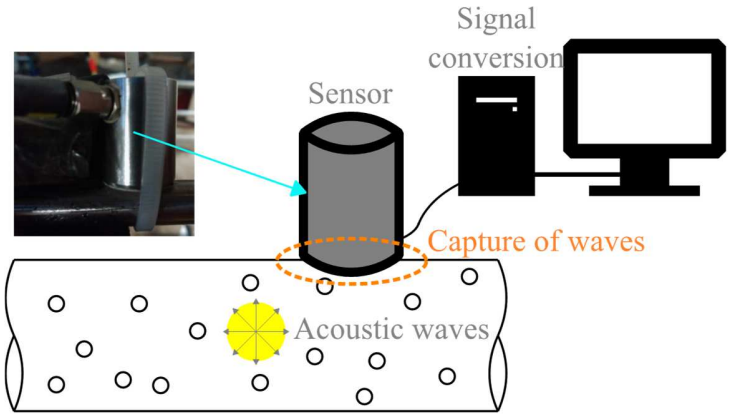

Figure 2. Acoustic emission sensor installed in the Archimede flow loop.

The position where the AE sensors are installed in the system are indicated in red in Figure 1. Four sensors were used (1A, 2B, 3C and 4A) in the tests presented. For each sensor, the number indicates the position in the system, while the letter indicates the nominal frequency: the type A are R15 sensors with a frequency of 150 kHz, type B is a PKBBI sensor with a frequency of 300 kHz, and type C is a WD sensor with a frequency of 350 kHz. The absolute energy is defined as the integration of the output voltage of the transducer over time during an acoustic emission hit divided by the electrical resistance of the measuring circuit (Cameirao et al., 2018). The parameters of the AE acquisition system chosen for the tests are indicated in Table 1.

Table 1. Characteristics of the AE sensors and acquisition.

Instrumentation	Characteristics and setup
Number of channels required for the test	4
Sensors type	R15, PKBBI, WD – Physical Acoustic Corporation
Resonant frequency	R15 (A): 150 kHz, PKBBI (B): 300 kHz, WD (C): 350 kHz
Analog filter	20-1000 kHz
Preamplifiers	30 dB
Acquisition time step	0.5 s
Peak definition time	200 µs
Hit definition time	800 µs
Hit lockout time	1000 µs

2.3 Experimental conditions and materials

The experiments are conducted at 4 °C and 75 bar (absolute pressure), using the following mixtures:

- Kerdane oil (C_{11} - C_{14} hydrocarbons).
- Saline water, with a concentration of 30 g of NaCl/L of deionized water.
- Natural gas (methane 91.7%, ethane 5.9%, propane 0.6%, carbon dioxide 0.8%, nitrogen 0.8%, i-butane 0.1%, n-butane 0.1%).

The volume of the liquid injected is 10.0 L at room pressure and temperature. Two tests were chosen among twenty-three for the analysis hereby presented: one at 30% water cut and another one at 80% water cut, at constant flow rate equal to 200 L/h.

3. Results and discussions

3.1 Detecting hydrate crystallization

For the first experiment, at 30% water cut and 200 L/h, Figure 3 shows the absolute energy for the four AE sensors, two temperatures, and the flow rate. The data from the different instruments are synchronized in time and space, meaning that the time it takes for a volume passing in a sensor to arrive to another sensor (dependent of the volume between the sensors and the flow rate) is considered for the plots. As indicated in the x-axis, the instrument used as reference is the Coriolis. One can see that, around 17.4 minutes, there is an increase of around two orders of magnitude in absolute energy for all the sensors (Figure 3(a)). This indicates hydrate formation, due to the collisions of particles that generates more noise,

as previously observed by Cameirao et al. (2018). This is confirmed in Figure 3(b), where the temperatures T_8 and T_9 increase around 18 minutes as a result of the exothermal process of hydrate formation. Hydrate formation provokes an oscillatory behavior in the flow rate, shown in Figure 3(c), when particles are suspended in the system. The flow rate also indicates that the system is no longer flowable around 30 minutes, when it is equal to zero, indicating plug. It is possible to see that the plugging was a sudden event because the flow rate was relatively stable at 200 L/h before became zero instantaneously. The plug was caused by the presence of large pockets containing hydrates while other parts of the flow contain only liquid. These pockets with hydrates are characterized by relatively large values of absolute energy, as observed in Figure 3(a), between the instants 20 and 30 minutes, while the regions with only liquid have the same level of absolute energy as before hydrate formation.

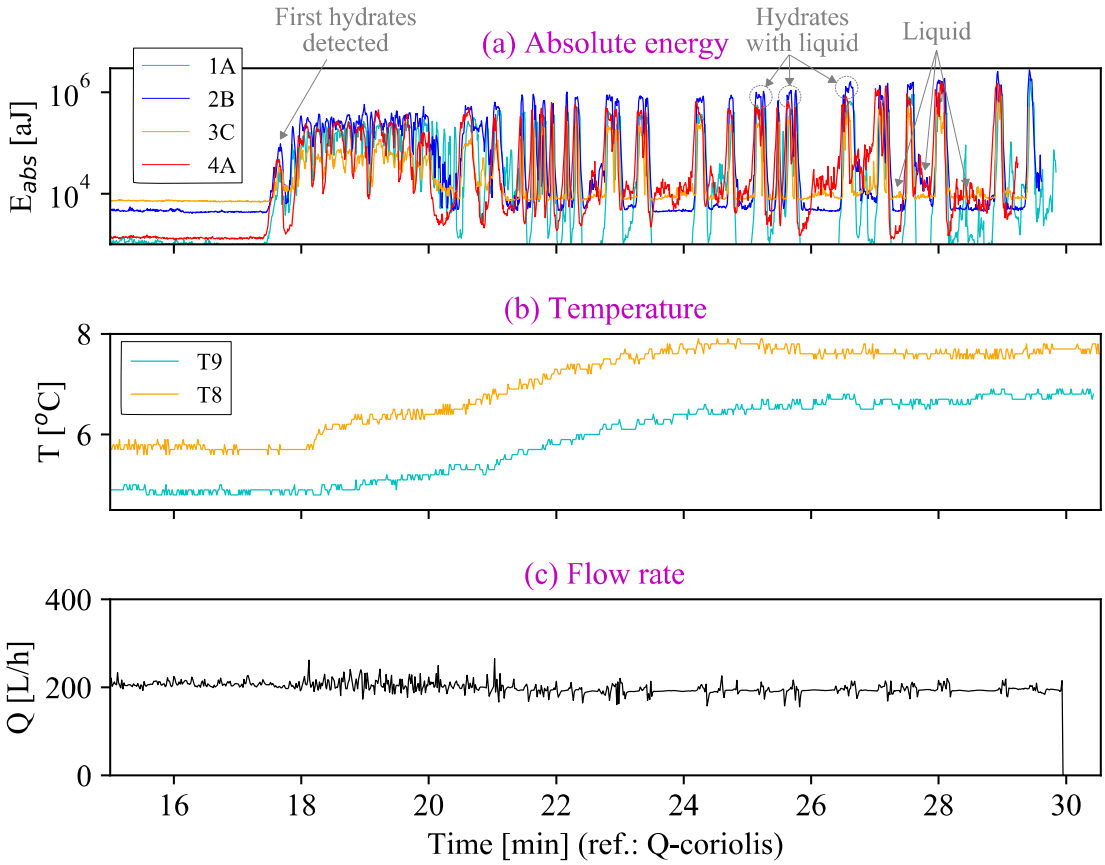

Figure 3. Experiment at 30% water-cut and 200 L/h, showing the: (a) absolute energies, (b) temperatures T_8 and T_9, and (c) measured flow rate.

The multi-instrumental methodology hereby presented allows detecting the position in the flow loop where there was initially a significant hydrate growth. Figure 4 shows the temperatures before and

after the pump and the absolute energies for all the AE sensors. The data now is not synchronized in space, in order to detect the spatial displacement of the hydrates. Around 16.6 minutes, the temperature T_8 (see Figure 4(a)) starts increasing, accusing hydrates passing in the position where the sensor is installed (after the pump). Less than a minute later, around 17.6 minutes, Figure 4(b) shows that the sensor 1A presents a sudden increase on the absolute energy, and then one by one of the other AE sensors also react, in sequence, with an increase of absolute energy. Finally, the last probe to detect an increase of the temperature was the sensor T_7, around 18.5 minutes, as shown in Figure 4(c). The results indicate that the position where hydrates initially formed was between the sensors T_7 and T_8. Indeed, the power provided by the pump may facilitate the local fluctuations of energy that allow hydrates to reach a stable size and grow. These results also confirm that the increase of the absolute energy is due to the hydrate slurry flow when hydrates pass in the position where each sensor is placed.

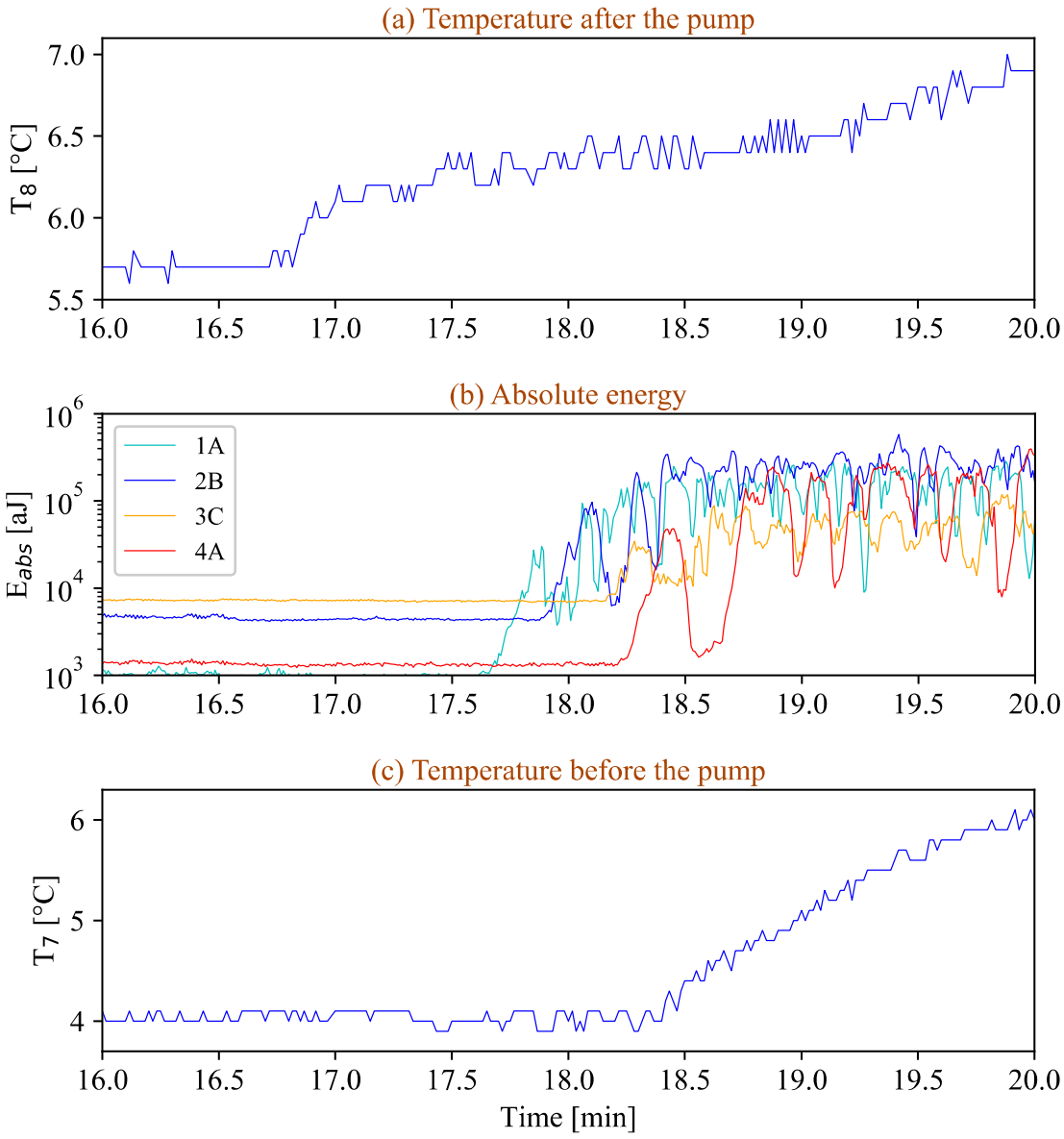

Figure 4. Detecting the onset of hydrate formation with temperature and absolute energy measurements for the test at 30% water cut and 200 L/h.

The AE system presents a great advantage compared to the temperature probes, which is its capacity to track the displacement of particles in space. From Figure 3(a) and Figure 4(b), it is clear that hydrates are not homogeneously distributed in space. Hydrate particles will concentrate in parts of the volume of the flow (regions at high absolute energy) leaving other parts only with liquid (values of absolute energy that are at the same level as before hydrates have formed). From the temperature measurement, it is possible to detect hydrate formation. However, the heat generated by the exothermal process is transferred to the liquid, preventing the detection of the displacement of hydrates by means of

the temperature measurement, and it is not possible to detect the local accumulations of hydrates in parts of the flowing volume.

Figure 5 shows the data of PVM, FBRM and absolute energy when hydrates are initially detected. The data is synchronized in space. The first PVM image to show hydrates is image 3 in Figure 5(a). These particles seem to be flowing dispersed in the liquid phase (dark background), while images 4-8 indicate that there are relatively large porous agglomerates passing in front of the PVM. The images 5-7 are very similar, which indicates that there was deposition on the instrument. The passage of the first particles (image 3) was not detected by the FBRM (Figure 5(b)), but it could be detected from the absolute energies (Figure 5(c)), which have a first peak when the particles seen in image 3 pass near the AE sensors.

The second peak observed on the absolute energy coincides with the arrival of the hydrates seen in the PVM (images 4-8). It is likely that there was also deposition on the FBRM instrument, since the number of counts remains approximately constant after the detection of hydrates (between 19.5 and 20.5 minutes), and it slightly decreases beyond 20.5 minutes.

The results indicate that immediately after hydrate formation, the phases started separating. There are regions with hydrates (peaks in absolute energy) and regions with liquid (absolute energy with the same values as before hydrate formation). This was previously observed in flow loop tests by Palermo and Sinquin (1997). One reason for this phase separation is the tendency of hydrates to trap the water phase, the sponge approach, proposed by Bassani et al. (2019). Another reason is the drift velocity between hydrate particles and liquid (the hydrates are slower than the liquid phase). Moreover, another reason can be the loss of kinetic energy of particles due to collision with the walls, or collision between particles. This mechanism is known as sloughing, which causes temporary accumulations due to non-permanent attachments of the particles to the wall. A combination of these three mechanisms is likely to be the reason for the separation of phases identified after hydrate formation, which forms a heterogeneous suspension, where some regions have more hydrates and other regions have liquid single-phase flow.

Despite the FBRM and PVM allow deducing many mechanisms of hydrate formation under flow (Melchuna et al., 2016), the use of AE presents the important advantage of tracking hydrate particles during the experiment, which cannot always be possible with the FBRM and the PVM. Since hydrates are porous structures, they may easily stick with surfaces of the instruments, and then they reduce the visibility of the images and may possibly form deposits in those intrusive instruments, affecting their measurements.

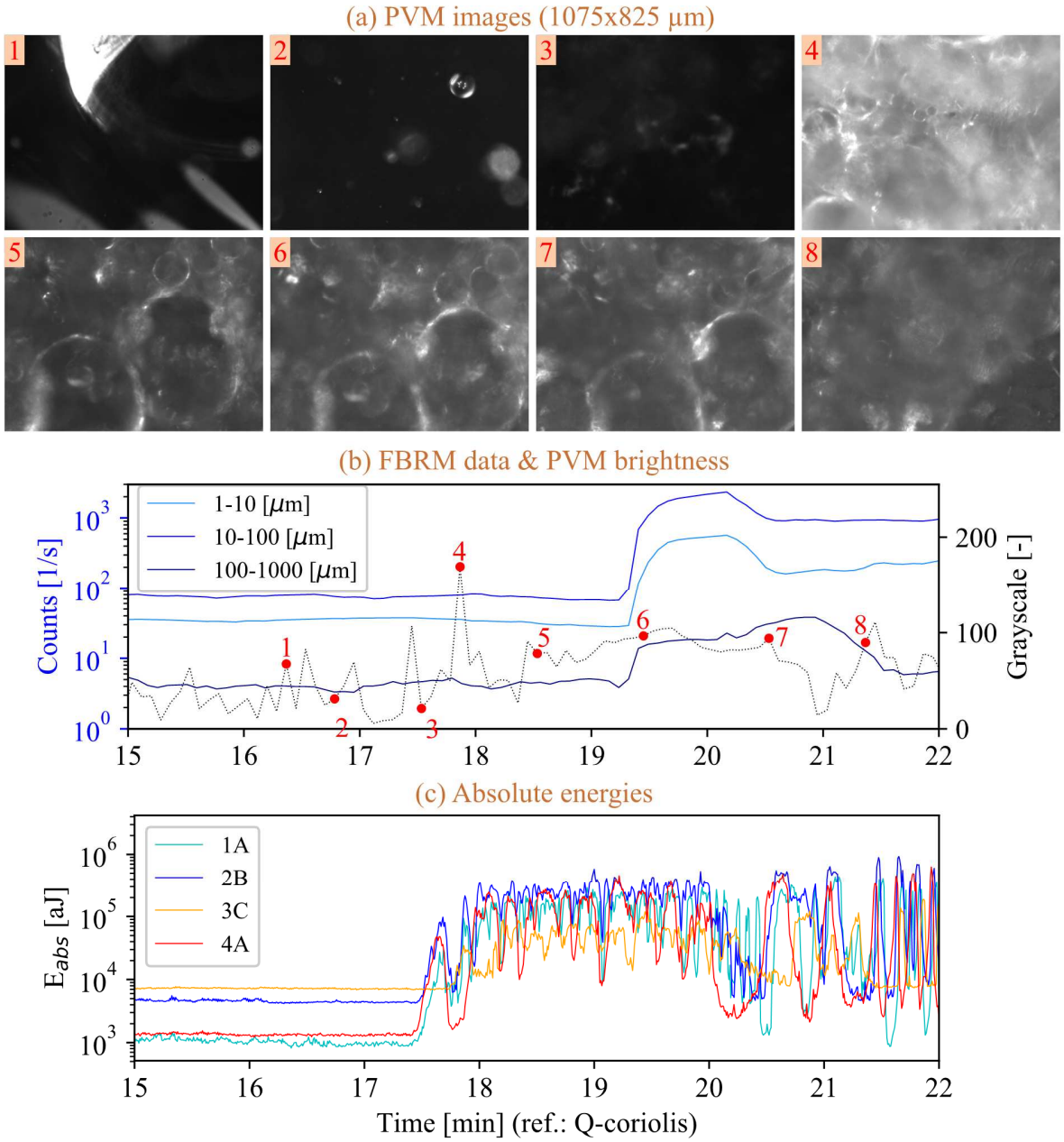

Figure 5. Onset of hydrate formation for the experiment at 30% water cut and 200 L/h, comparing (a) the PVM images, (b) chord counts and PVM-brightness, and (c) absolutes energies.

For the experiment at 80% water cut it is shown in Figure 6(a) that, the absolute energy increases continuously between 3 and 10 minutes, presenting some small oscillations. During the same interval, the flow rate is perturbed, as shown in Figure 6(b), which indicates a significant hydrate formation during this interval. Then the oscillatory behavior with the flow rate reduces, while the absolute energy starts

presenting an intermittent behavior with large values followed by low values of absolute energy. Such intermittence presents a period of approximately 2.5 minutes.

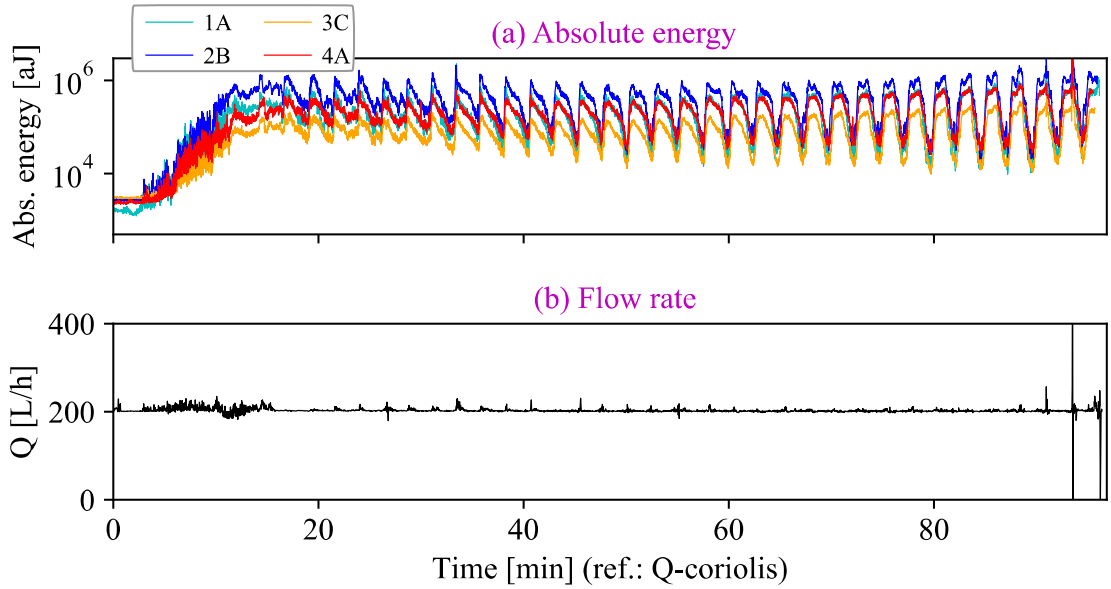

Figure 6. Experiment at 80% water-cut, 200 L/h, showing the: (a) absolute energies, and (b) flow rate.

To better understand how the AE signals responded to hydrate crystallization for the test at 80% water cut, the data from the first 20 minutes of the experiment is shown in Figure 7. The first hydrates can be seen in image 2, from the PVM-images in Figure 7(a). Once hydrates form, the absolute energy (Figure 7(c)) gradually increases. The absolute energies from all the sensors present oscillations between 3 minutes, which is the onset of hydrate formation, and 11 minutes. This interval coincides with the small particle suspension seen in the PVM-images 2-4. In addition, between 3 and 11 minutes, there was no detectable increase on the temperature (Figure 7(d)), meaning that the volume of hydrates formed was not enough to increase the temperature. A change in the flow regime occurred around 11 minutes, where larger hydrate particles can be seen with the PVM. The oscillations on the absolute energy decrease with the increase of temperature. For this experiment, the initial hydrate formation, which occurred at microscopic level, was not detectable by an increase of the temperature, but it was observable from the PVM images and from the absolute energy, showing a gradual hydrate growth until 11 minutes. After that, particles of larger sizes are detected (images 5 e 6 in Figure 7(a)), which can be confirmed by the grayscale of the PVM images shown in Figure 7(b). The chord counts for the group 100-1000 µm also increased around the same time, around 11 minutes.

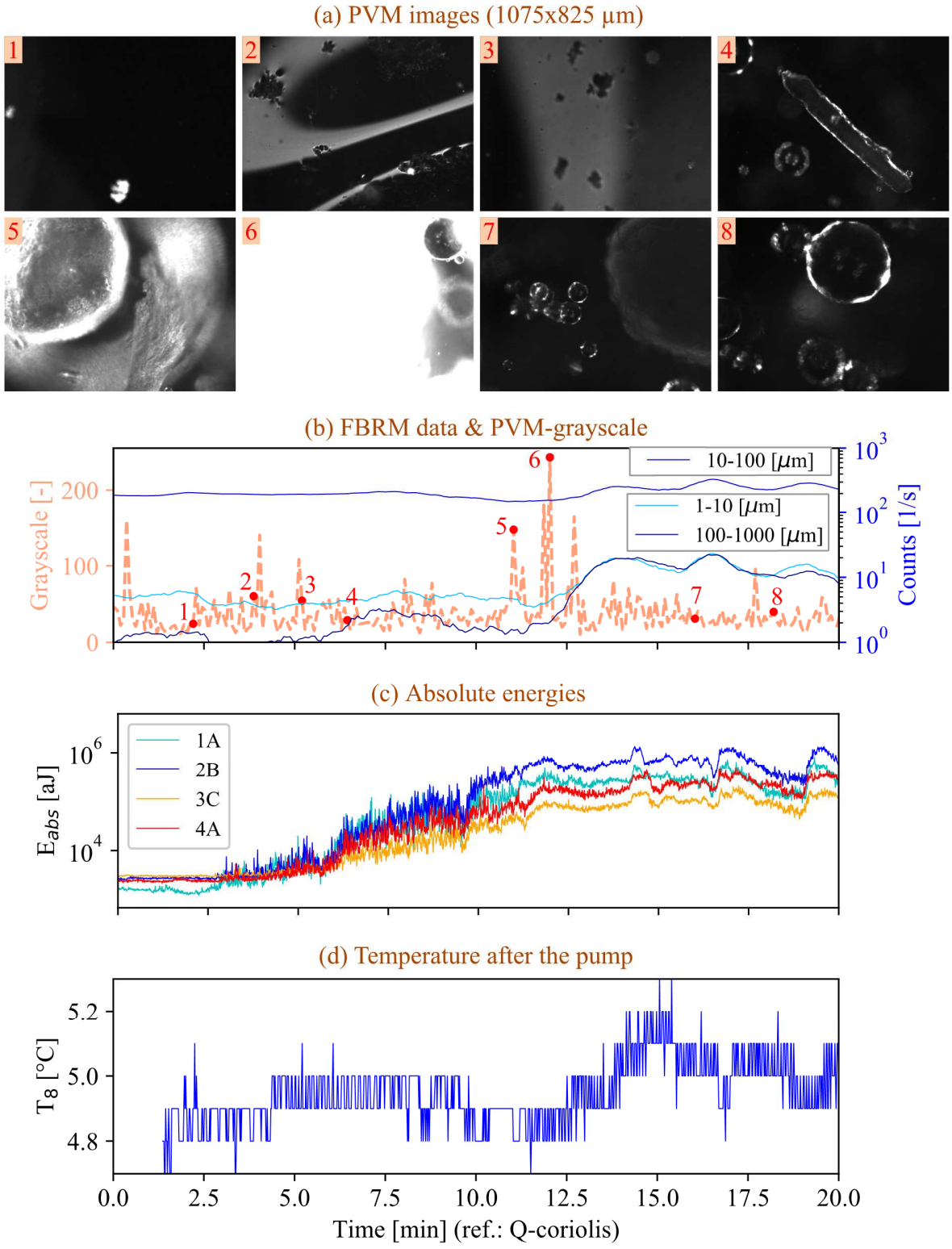

Figure 7. Detection of hydrate formation for an experiment at 80% water-cut by comparing the (a) PVM images, (b) chord length counts with PVM images grayscale, (c) absolute energies, and (d) temperature.

Figure 8 shows some images from the camera compared to the absolute energy captured from the AE sensor installed near the visualization window. Based on both information, it is possible to separate the beginning of hydrate formation and growth into three the different steps:

i. Once hydrates start forming, they form on oil surfaces. One can notice that because the droplets become darker once hydrates start forming (image 2, Figure 8(a)), when compared to the image of the flow before hydrate formation (image 1). This beginning of hydrate formation causes a slightly increase on the absolute energy (before the instant 6.5 minutes, Figure 8(b)).

ii. As the flow continues circulating around the loop, small hydrate particles break and detach from the oil surfaces. One can notice that because the image 3 becomes darker, even in regions where it is not possible to see particles with a defined shape (bottom of the image). During this step observed in image 3, the absolute energy increases once again, and it starts oscillating more than during the previous step, which indicates the continuous hydrate formation and breakage of particles.

iii. The flow becomes more stable, with relatively large particles (several millimeters, that can be seen in the image) dispersed in the liquid. This can be seen in last image (image 4, Figure 8(b)), showing the flow regime once the small oscillations of absolute energy are over.

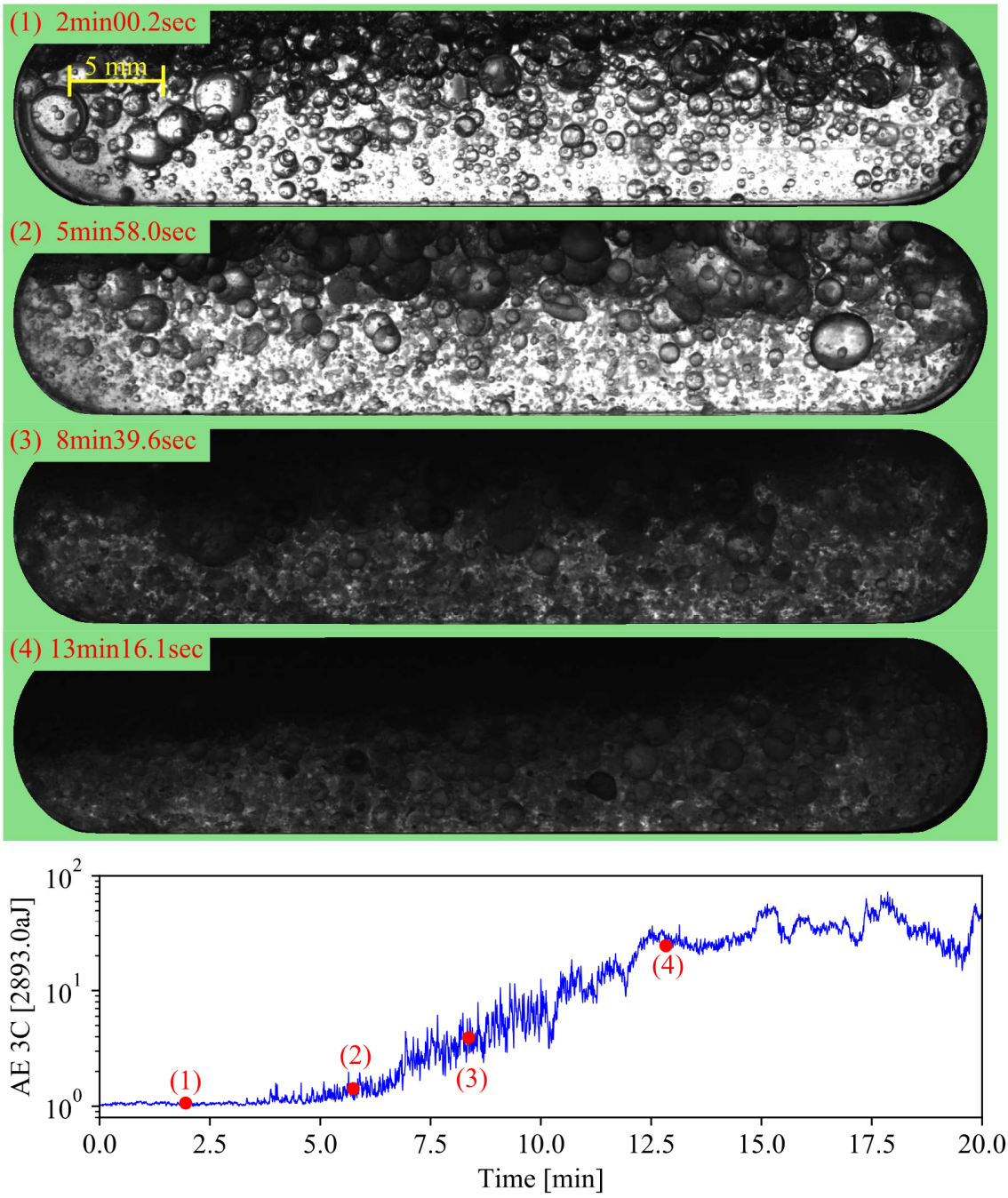

Figure 8. Comparison between the images from the camera and the absolute energy measured near the window for the test at 80% water-cut and 200 L/h.

3.2 Identifying and quantifying deposition or local accumulations with AE

Another application of AE is the non-flowing volume, which can be due to deposition of local accumulations in the system. As discussed previously, the AE sensors detect flowing hydrates due to the

energy dissipation caused by collisions. Therefore, hydrates that are not flowing due to deposition or local accumulations cannot be detected. Quantifying the interval of time that it takes for the particles to give a turn around the loop allows the estimation of the total fraction of the mixture (oil, water and hydrates) that is not flowing. The total flowing volume (V_f) of liquid with hydrates during the time interval for a turn around the loop (Δt_{lap}) can be calculated with the flow rate measured by the Coriolis, that is, $V_f = \sum_{\Delta t_{lap}} Q \cdot \Delta t$. The volume of hydrates formed is calculated from the gas consumed for hydrate formation, obtained from the gas injected in the system to maintain the pressure constant.

For the test at 30% water cut, the absolute energy for the sensor 2B during two turns around the loop is shown in Figure 9. The flowing volume calculated during each one of the two intervals was approximately 7.39 liters. Considering that the final volume of liquid with hydrates in the system is 10.72 liters, the estimated non-flowing volume is 31.1%.

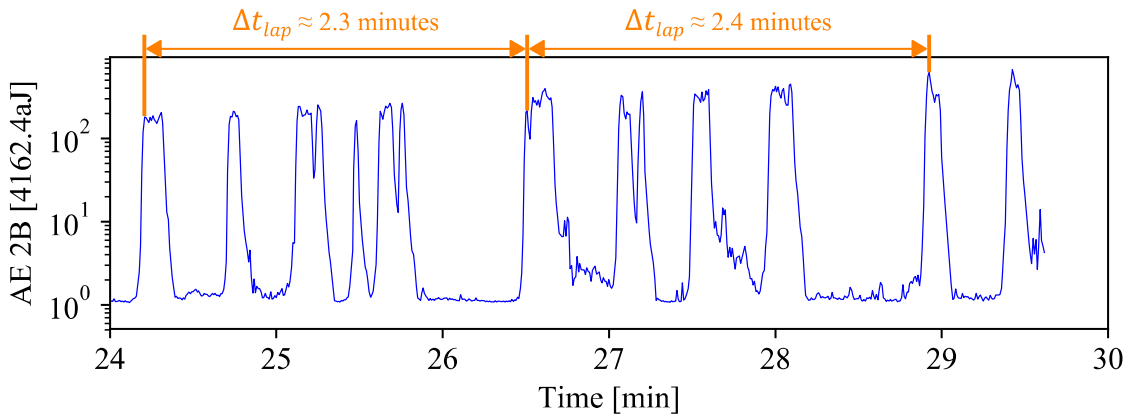

Figure 9. Absolute energy during two laps in the flow loop for the test at 30% water cut.

Applying the same procedure for the test at 80% water cut, Figure 10 shows the absolute energy from the sensor 3C during two laps around the loop. The flowing volume during those two intervals was approximately 8.28 liters, indicating that the non-flowing volume is around 1.95 out of 10.23 liters. It corresponds to approximately 19.0 % in volume of deposition or local accumulations.

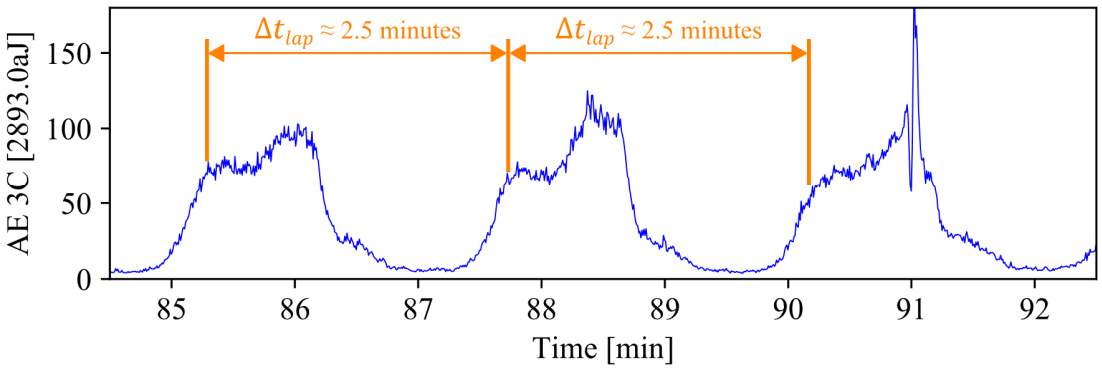

Figure 10. Absolute energy during two laps in the flow loop for the test at 80% water cut.

4. Conclusions

An application of AE technology in flow loop tests with gas hydrates formation under multiphase flow was presented in this work. It was shown that the absolute energy captured by a sensor increases as hydrates flow in front of the sensor. Consequently, it can be used to track hydrate particles in space. AE presents some advantages compared to other instruments. First, it is non-intrusive, and therefore, it does not disturb the flow or cause any local accumulations. AE is also more sensitive to crystallization than the other probes tested, especially the temperature. In addition, it allows differentiating regions of the liquid flow with or without hydrates. The other instruments do not allow following the hydrate particles in space.

AE enables detecting and quantifying the non-flowing volume due to deposition or local accumulations in singularities. This is possible by monitoring the turns around the loop and measuring the interval of time for each turn. By integrating the flow rate over time, it is possible to calculate the total flowing volume, and consequently, the fraction of the mixture that does not flow.

An important observation was that the flow pattern rearranges after hydrate formation in a way that there is a separation into two main regions: one with liquid and another one with liquid and hydrates. The hydrate particles accumulation in parts of the liquid volume can be detected by AE, forming large pockets containing hydrates and entrapped liquid, which may be an important cause of plugging. This mechanism will be further investigated and explained in future works. Furthermore, advancements in the application of this technique with AE will further allow quantifying the local hydrate fractions in the system.

AKNOWLEDGEMENTS

The authors would like to acknowledge the financial support received from Total Energies in the framework of the project Archimede 5. We also would like to thank the technical support provided by members of the SPIN center at Mines Saint-Etienne, especially Mr. F. Chauvy and Mr. H. Faure for the technical assistance with the flow loop apparatus.

REFERENCES

Al-Lababidi, S., Mba D., Addali, A., 2012. Upstream Multiphase Flow Assurance Monitoring Using Acoustic Emission. 10.5772/31332.

Aman, Z.M., Di Lorenzo, M., Kozielski, K., Koh, C.A., Warrier, P., Johns, M.L., May, E.F., 2016. Hydrate formation and deposition in a gas-dominant flowloop: Initial studies of the effect of velocity and subcooling. J. Nat. Gas Sci. Eng., 35, 1490-1498.

Bassani, C.L., Melchuna, A.M., Cameirao, A., Herri, J-M, Morales, R.E.M., Sum, A.K., 2019. A Multiscale Approach for Gas Hydrates Considering Structure, Agglomeration, and Transportability under Multiphase Flow Conditions: I. Phenomenological Model. Ind. Eng. Chem. Res., 58, 14446-14461.

Cameirão, A., Serris, E., Melchuna, A., Herri, J-M., Glenat, P., 2018. Monitoring gas hydrate formation and transport in a flow loop with acoustic emission. J. Nat. Gas Sci. Eng., 55, 331-336.

Cardoso, C.A.B., Gonçalves, M.A.L., Camargo, R.M.T., 2014. Design Options for Avoiding Hydrates in Deep Offshore Production. J. Chem. Eng. Data, 60, 330-335.

Deka, B., Barifcani, A., Al Helal, A., Badi, D., Mahto, V., Vuthaluru, H., 2021. Generation of methane gas hydrate equilibrium curve for the thermodynamic gas hydrate inhibitor propylene glycol. J. Pet. Sci. Eng., 199, 108312.

Ding, L., Shi, B., Lv, X., Liu, Y., Wu, H., Wang, W., Gong, J., 2016. Investigation of natural gas hydrate slurry flow properties and flow patterns using a high pressure flow loop. Chem. Eng. Sci. 146, 199-206.

Droubi, M.G., Reuben, R.L., White, G., 2015. Monitoring acoustic emission (AE) energy in slurry impingement using a new model for particle impact. Mechanical Systems and Signal Processing, Volumes 62–63, 2015, p. 415-430.

Droubi, M.G., Reuben, R.L., 2016. Monitoring acoustic emission (AE) energy of abrasive particle impacts in a slurry flow loop using a statistical distribution model. Applied Acoustics, Volume 113, 202-209.

El-Alej, M.E., Corsar, M., Mba, D., 2014. Monitoring the presence of water and water-sand droplets in a horizontal pipe with Acoustic Emission Technology. Appl. Acoust. 82, 38–44.

El-Alej, M., Mba, D., Yan, T., Alssayh, M., 2013. Identification of minimum transport condition for sand in two-phase flow using acoustic emission technology, Applied Acoustics, 74, 1266-1270.

Fang, L., Liang, Y., Lu, Q., Li, X., Liu, R., Wang, X., 2013. Flow noise characterization of gas–liquid two-phase flow based on acoustic emission. Measurement, 46, 3887-3897.

Fidel-Dufour, A., Gruy, F., Herri, J.M., 2006. Rheology of methane hydrate slurries during their crystallization in a water in dodecane emulsion under flowing. Chem. Eng. Sci., 61, 505-515.

Gherras, N., Serris, E., Fevotte, G., 2012. Monitoring industrial pharmaceutical crystallization processes using acoustic emission in pure and impure media. Int. J. Pharm., 439, 109-119.

Hii, N.C., Tan, C.K., Wilcox, S.J., Chong, Z.S., 2013. An investigation of the generation of Acoustic Emission from the flow of particulate solids in pipelines. Powder Tech. 243, 120-129.

Husin, S., Addali, A., Mba, D., 2013. Feasibility study on the use of the Acoustic Emission technology for monitoring flow patterns in two phase flow. Flow Meas. Instrum., 33, 251-256.

Joshi, S.V., Grasso, G.A., Lafond, P.G., Rao, I., Webb, E., Zerpa, L.E., Sloan, E.D., Koh, C.A., Sum, A.K., 2013. Experimental flowloop investigations of gas hydrate formation in high water cut systems. Chem. Eng. Sci., 97, 198-209.

Kinnari, K., Hundseid, J., Li, X., Askvik, K.M., 2015. Hydrate Management in Practice. J. Chem. Eng. Data, 60, 437-446.

Liu, Z., Yang, M., Zhang, H., Xiao, B., Yang, L., Zhao, J., 2019. A high-pressure visual flow loop for hydrate blockage detection and observation. Rev. Sci. Instrum. 90, 074102.

Liu, Z., Farahani, M.V., Yang, M., Li, X., Zhao, J., Song, Y., Yang, J., 2020. Hydrate slurry flow characteristics influenced by formation, agglomeration and deposition in a fully visual flow loop. Fuel, 277, 118066.

Liu, Z., Liu, Z., Wang, J., Yang, M., Zhao, J., Song, Y., 2021. Hydrate blockage observation and removal using depressurization in a fully visual flow loop. Fuel, 294, 120588.

Melchuna, A., Cameirao, A., Herri, J.M., Glenat, P., 2016. Topological modeling of methane hydrate crystallization from low to high water cut emulsion systems. Fluid Phase Equilib., 413, p. 158-169.

Nasir, Q., Suleman, H., Elsheikh, Y.A., 2020. A review on the role and impact of various additives as promoters/inhibitors for gas hydrate formation. J. Nat. Gas Sci. Eng., 76, 103211.

Olajire, A.A., 2020. Flow assurance issues in deep-water gas well testing and mitigation strategies with respect to gas hydrates deposition in flowlines-A review. J. Molecular Liquids, 318, 114203.

Palermo, T., Sinquin, A., 1997. Pilot Loop Tests of New Additives Preventing Hydrate Plugs Formation. In: Multiphase 97, 8th International Conference on Multiphase Flow, 133-137.

Pham, T.K., 2018. Experimental study and modelling on methane hydrates crystallization under flow from a water-oil dispersion at high water cut. PhD Thesis, 334 p., Mines Saint Etienne, France.

Qasim, A.; Khan, M.S., Lal, B., Ismail, M.C., Rostani, K., 2020. Quaternary ammonium salts as thermodynamic hydrate inhibitors in the presence and absence of monoethylene glycol for methane hydrates. Fuel, 259, 116219.

Sloan, E.D., 2005. A changing hydrate paradigm – from apprehension to avoidance to risk management. Fluid Phase Equilib., 228-229, 67-74.

Sloan, E.D., Koh, C.A., 2008. Clathrate Hydrates of Natural Gases - 3rd edition. CRC Press Inc.

Sloan, E.D., Koh, C.A., Sum, A.K., 2011. Natural Gas Hydrates in Flow Assurance. GPP – Elsevier.

Yan, K.L., Sun, C.Y., Chen, J., Chen, L.T., Shen D.J., Liu, B., Jia, M.L., Niu, M., Lv, Y.N., Li, N., Song Z.Y., Niu, S.S., Chen, G.J., 2014. Flow characteristics and rheological properties of natural gas hydrate slurry in the presence of anti-agglomerant in a flow loop apparatus. Chem. Eng. Sci., 106, 99-108.